1 - THE CELESTIAL SYSTEM AND FRAME OF IERS

Introduction

The celestial reference frame of IERS is based on the positions of compact extragalactic objects measured by VLBI. It is maintained on the basis of the analyses of several observation programs for the study of Earth rotation, crustal deformations, astrometry, and for deep space navigation. We present hereafter its latest realization, which is a combination of the individual frames obtained independently by two groups. The GSFC frame (Ma *et al.*, 1991), includes 334 objects observed with various networks: the International Radio Interferometric Surveying (IRIS), the NASA Crustal Dynamic Project (CDP), the Navy VLBI Network (NAVNET), and in the Naval Research Laboratory (NRL) reference frame program. The JPL frame (Steppe *et al.*, 1991) gives the positions of 241 objects observed with Deep Space Network. The two frames have 179 objects in common. The combination is based on a three rotation angle model applied to a selection of radio sources common to the individual frames. The initial definition of the system and the maintenance process is described by Arias and Feissel (1990); the connection to the conventional terrestrial system of IERS at the level of 0.001" is studied by Feissel (1991).

The distribution on the sky of the latest realization (IERS, 1991) of the IERS celestial reference system is shown on figure 1; the declination interval covered is from -84° to +85°.

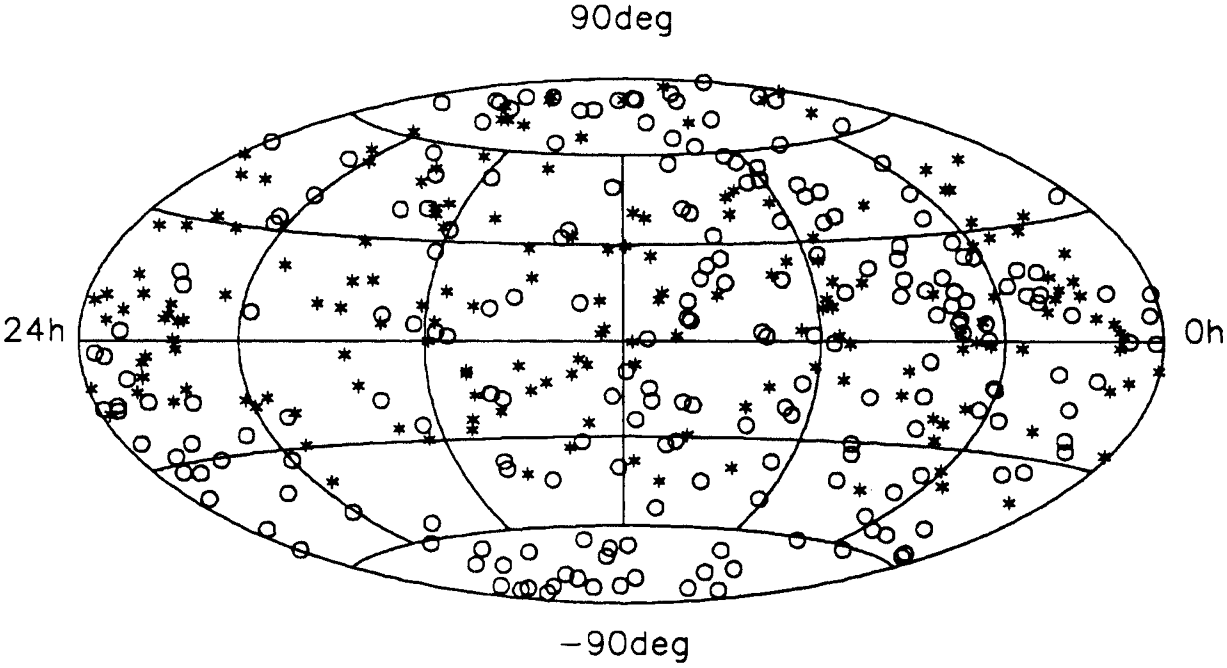

Figure 1. Distribution of the 396 extragalactic radio sources of RSC(IERS)91 C 01.
The asterisks show the objects observed independently in two programs (DSN, and IRIS/CDP/NAVNET/NRL).

The observational history and the physical properties of the sources are described in section 2, this volume. The redshifts span the interval 0.1-2.5 quite evenly. The total flux is in general over 1 Jansky. The spectral indices are between -0.8 and +1.4. The distribution in optical magnitudes has a peak around the 18th magnitude. A part of the IERS sources has been mapped at S and X bands (e.g. Charlot 1990). The primary sources mapped show no significant structure at the angular scale of 0.001".

Internal consistency and precision of the frame

It is well known that the use of the conventional IAU 1976 Precession and IAU 1980 Theory of Nutation in the analysis of VLBI observations would give rise to systematic errors in the source positions, and to misorientation of the axes of the frames, both at the level of a few milliarcseconds. Therefore the common practice in catalogue work is to estimate additional parameters which describe the motion of the celestial pole relative to its conventional position, either by estimating celestial pole offsets for each session, or by estimating a precession correction and the residual amplitudes of some of the nutation terms, as allowed by the length and time density of the series of observations analysed. Sovers (1991a) studies in detail the effects of these procedures on the resulting source positions. In the combination performed by the Central Bureau of IERS, only individual frames obtained by one of these procedures are used. The slight offsets between the poles of the catalogues, that are due to inconsistent fixing of the celestial pole offsets at some reference day, are accounted for by the adjustment of rotation angles; they have no influence on the consistency of the individual frames with the combined one.

The noticeably different network geometries of the various observing programs are expected to cause regional deformations in the derived celestial frames. From detailed comparisons of large JPL and GSFC catalogues, Sovers (1990) concludes that the only systematic difference between the two catalogues is an increase of right ascension differences for lower declinations, amounting to 0.001" to 0.002" over the entire range of declinations.

A detailed analysis of the internal consistency and precision of the frame is given in section 2, this volume.

Definition and maintenance of the system

The IERS celestial reference system is barycentric through the appropriate modelling of observations by the analysis centres which contribute individual catalogues. The condition that the sources have no proper motion is also applied by the analysis centres; however, checks are regularly performed to insure the validity of this constraint (Ma and Shaffer, 1991) to avoid spurious motions of some sources.

The direction of the axes of the IERS celestial reference system is illustrated on Figure 2, which represents estimated positions of the FK5 and IERS polar axes relative to the mean celestial pole at J2000.0, and estimated relative positioning of the FK5 and IERS right ascension origins. The estimated parameters are rotation angles A_1, A_2, A_3, around three axes in the directions $\alpha = 0^h$, $\delta = 0$; $\alpha = 6^h$, $\delta = 0$; $\delta = 90°$. A_1, A_2 are plotted in a plane tangent to the celestial sphere at the celestial pole; A_3 is plotted in a plane tangent to the celestial sphere in the vicinity of the equinox.

The Ox axis was implicetely defined in the initial realization (Arias *et al.*, 1988b) by the adoption of the right ascensions of 23 radio sources in catalogues obtained by the GSFC, the JPL, and the NGS. These catalogues had been compiled by fixing the right ascension of 3C273B to the usual (Hazard *et al.* 1971) conventional FK5 value (12h 29m 6.6997s at J2000.0). The figure shows the positions of the IERS and FK5 origins relative to the dynamical equinox at J2000.0. The uncertainty on the FK5 origin of right ascensions is derived from the quadratic sum of the accuracies given by Fricke, (1982) (±0.045") and Schwann, (1988) (±0.07"/cy), considering a mean epoch of

1955 for the proper motions in right ascensions. Comparing VLBI and LLR Earth orientation and terrestrial frames shows that the IERS origin of right ascensions is consistent with the dynamical equinox of the JPL ephemeris DE200 within 0.01" (Finger and Folkner 1992, Charlot 1991).

The Oz axis points in the direction to the mean pole at J2000.0 as defined by the IAU conventional models for precession and nutation. As a result of the inaccuracy of the conventional models, the Oz axis of the IERS celestial system is shifted from the expected position of the mean pole at J2000.0 by about 0.01" in longitude sin ε and 0.001" in obliquity. In the figure, the coordinate axes are centered at the mean celestial pole at J2000. P_{IERS} is an estimation of the IERS polar axis derived from VLBI analyses (e.g. Steppe *et al.*, 1991); the various VLBI estimations agree within a few milliarcseconds (radius of the circle around P_{IERS}). The area of probable position of the FK5 pole is obtained by first considering that the systematic part is dominated by a correction of -0.25"/cy to the precession constant imbedded in the FK5 System, and second by adopting Fricke's (1982) estimation of the accuracy of the FK5 equator (±0.02"), and Schwan's (1988) estimation of the limit of the residual rotation (±0.07"/cy), taking the epochs of observations from Fricke *et al.*, (1988). If one assumes that the error in the precession rate is absorbed by the proper motions of stars, the circle has to be centered at P_{J2000}, keeping the same radius.

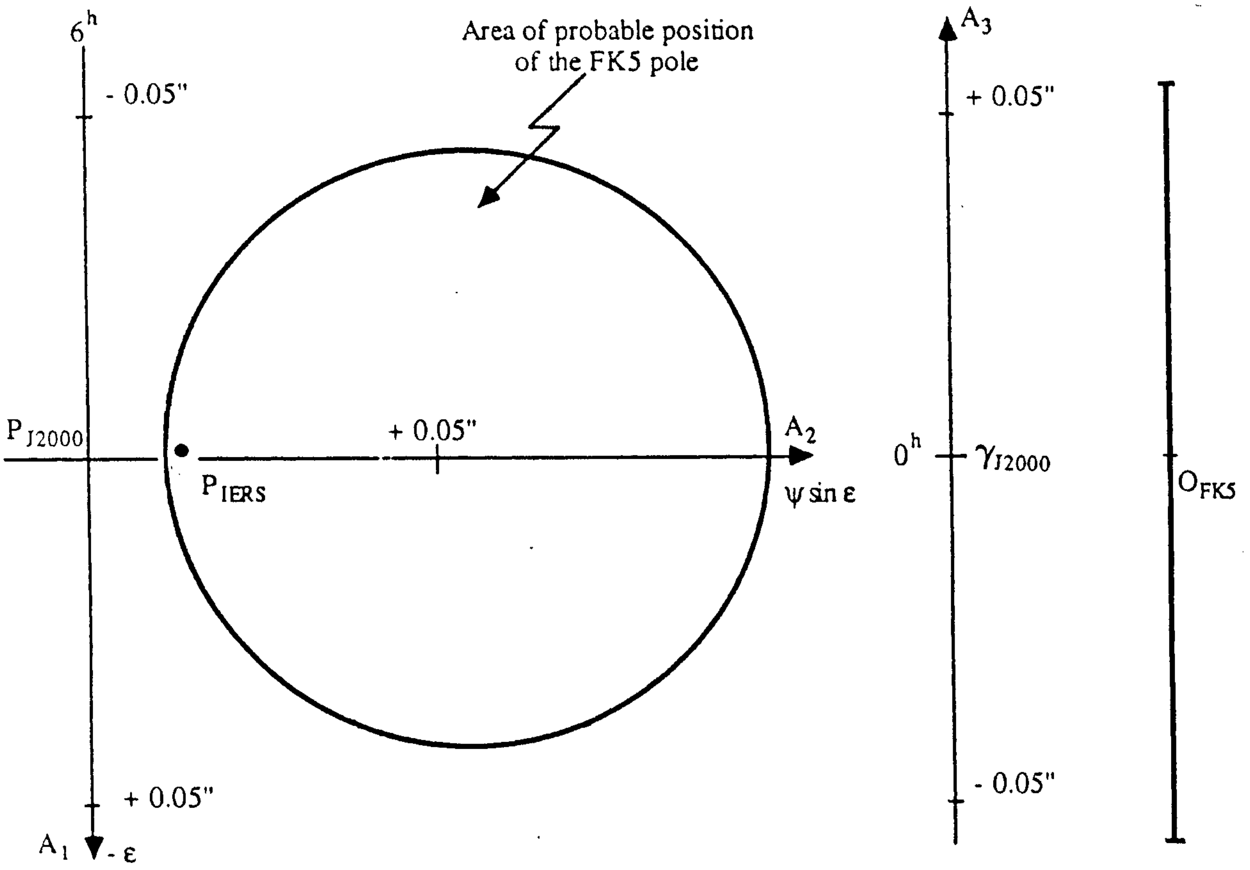

Figure 2. Direction of the axes of the IERS and FK5 celestial systems relative to the mean pole and equinox at J2000.0.

The new astrometric techniques and the availability of large computers used to analyze data raise the question of how one should understand the conventional character of the celestial frame. In practice, it can be understood in two ways:

- the source coordinates themselves are considered conventional, *i.e.*, their numerical values are fixed for some time (years); this is the FKn philosophy,

- the axes of the system are considered conventionally as fixed to their initial directions, but improved or additional source coordinates available at the time of analysis are provided to the users; this is required for space navigation, Earth orientation programs, geodetic applications, linkage of celestial frames, etc. The system maintenance method applied by the Central Bureau of IERS is along these lines; it should be mentioned that such a procedure is made possible by the high model standardization in the operation of IERS, and by the fact that the implementation of an extragalactic celestial frame implies much less geophysical and astronomical modelling than does the FK series of catalogues. This approach was also retained in the IAU resolutions on reference systems, adopted in August 1991 (see Table 1).

New realizations of the IERS celestial reference system are produced whenever justified by the progress in the observations or in the modelling. The successive realizations produced up to now have maintained the initial definition of the axes within 0.0001"; the coordinates of the 57 primary sources have changed by less than 0.0006" (rms).

At its 1991 General Assembly, the International Astronomical Union has made recommendations on the future conventional celestial system for astronomical research, listed in Table 1. The analyses of the IERS celestial system presented in section 2, this volume, and of its tie with the HIPPARCOS celestial frame (section 3) should help to make clear the contribution of IERS to the future conventional celestial reference system.

Physical properties and observational history of the fiducial objects

The physical properties of the 396 radio sources in RSC(IERS)91 C 01 can be investigated on the basis of a VLBI survey published by Preston *et al.* (1985). The survey was conducted by performing 2.29 GHz VLBI observations over the full sky. The result is a catalogue of 1398 objects with the following information : redshift, total flux, spectral index, optical identification and visual magnitude. The characteristics of the IERS sources are listed in Tables 2 (p. 10) and 3 (p. 14), together with the numbers of observations and formal uncertainties of the coordinates.

Figures 3a through 3d (pages 19-22) show the histograms of the optical identifications, visual magnitudes, redshifts and total radio flux of sources in the last realisation of IERS celestial reference frame.

The distribution of visual magnitudes of IERS objects (Figure 3b, Table 5) is similar to the one in the survey, with a peak around the 18th magnitude. The total radio fux (Figure 3c, Table 6) is in general over 1 Jansky, while the survey has a larger proportion of weaker radio sources. The redshifts (Figure 3d, Table 7) are quite evenly distributed in the interval 0.1-2.5.

Table 1. IAU Resolution A4: recommendations VI and VII from the Working Group on Reference Systems (1991)

RECOMMENDATION VI

considering,

the desirability of implementing a conventional celestial barycentric reference system based upon the observed positions of extragalactic objects, and,

noting,

the existence of tentative reference frames constructed by various institutions and combined by the International Earth Rotation Service (IERS) into a frame used for Earth rotation series,

recommends,

1. that intercomparisons of these frames be extensively made in order to assess their systematic differences and accuracy,
2. that an IAU Working Group consisting of members of Commissions 4, 8, 19, 24, 31 and 40, the IERS, and other pertinent experts, in consultation with all the institutions producing catalogs of extragalactic radio sources, establish a list of candidates for primary sources defining the new conventional reference frame, together with a list of secondary sources that may later be added to or replace some of the primary sources, and,

requests,

1. that such a list be presented to the XXIInd General Assembly (1994) as a part of the definition of a new conventional reference system,
2. that the objects in this list be systematically observed by all VLBI and other appropriate astrometric programs.

Note for Recommendation VI

This recommendation essentially describes the first part of the work that must be done to prepare the realization of the reference system defined by Recommendations I and II. The choice of objects must be made in the first place by considering their observability by VLBI, but special care should be taken to include a large proportion of extragalactic radio sources with well identified optical counterparts.

Table 1. (cont.)

RECOMMENDATION VII

considering,

a) that the new conventional celestial barycentric reference frame should be as close as possible to the existing FK5 equator and equinox and the dynamical equinox which are referred to J2000.0,

b) that it should be accessible to astrometry in visual as well as in radio wavelengths,

recommends,

1. that the principal plane of the new conventional celestial reference system be as near as possible to the mean equator at J2000.0 and that the origin in this principal plane be as near as possible to the dynamical equinox of J2000.0,
2. that the positions of the extragalactic objects selected in accordance with Recommendation VI and representing the reference frame be computed initially for the equator and equinox J2000.0 using the best available values of the celestial pole offset with respect to the IAU expressions for precession and nutation,
3. that a great effort be made to compare reference frames of all types, in particular the FK5, solar system and extragalactic reference frames,
4. that observing programs be undertaken or continued in order to relate planetary positions to radio and optical objects, and to determine the relationship between catalogs of extragalactic source positions and the best catalogs of star positions, in particular the FK5 and Hipparcos catalogs.

Table 1. (cont.)

Notes for Recommendation VII

1. *This recommendation specifies the choice of the coordinate axes that will be adopted in the final reference frame and describes the work to be done before such a frame can be constructed. Although the considerations call for visual and radio wavelengths for the primary catalog, other observable wavelengths are not excluded. Positions of objects observed in other wavelengths should also be referred to the same system.*

2. *The objective set by this recommendation is that there should be no discontinuity in the positions of stars when the present FK5 frame is replaced by the extragalactic reference frame. This means that the position of the extragalactic objects should be in the FK5 system for J2000.0. It is acknowledged that the best values of precession and nutation must be used in order to avoid introducing spurious proper motions into the positions of extragalactic objects. The final transfer to the preferred equinox and principal plane will be done by applying a rotation at J2000.0.*

3. *The dynamical equinox in this recommendation is defined as the intersection of the mean equator and the ecliptic. The latter is defined as the uniformly rotating plane of the orbit of the Earth-Moon barycenter averaged over the entire period for which the ephemerides are valid. Since it is ephemeris dependent, the choice of the equinoctial point will be made using the most accurate and generally available ephemerides of the solar system at the time.*

4. *The definition given to the reference system by Recommendations I and II implies the stability in time of the system of coordinates realized by the celestial reference frame. The directions of the coordinate axes should not be changed even if at some later date the realization of the dynamical equinox or CEP are improved. Similarly, modifications to the set of extragalactic objects realizing the reference system should be made in such a way that the directions of the axes are not changed. This means that once the coordinate axes have been specified, in the way described in the first part of the recommendation, the connection between the definition of the conventional reference system and the peculiarities of the Earth's kinematics will have been severed.*

5. *As long as the relationship between the optical and the extragalactic radio frames is not sufficiently accurately determined, the FK5 catalog shall be considered as a provisional realization of the celestial reference system in optical wavelengths.*

Table 2. Characteristics of the objects in the IERS Celestial Reference Frame.
Objects observed by at least two programs.

OBJECT	Tp (1)	Redsh.	Flux (Jy)	SP	m_V	GSFC soln Nobs	JPL soln Nobs	IERS σ_α (2)	σ_δ (3)
0003-066	G	0.347	1.69	0.0	19.7	12	3	0.49	13.28
0008-264	Q	1.096	0.58	0.3	19.0	8	40	0.97	0.68
0016+731	Q	-	1.50	0.2	18.2	1583	11	0.81	0.24
0048-097	B	-	1.30	0.8	17.3	694	25	0.16	0.31
0104-408	Q	-	-	0.6	19.0	65	119	0.19	1.11
0106+013	Q	2.107	3.90	0.5	18.4	16716	273	0.16	0.27
0111+021	A	0.047	-	-0.2	16.5	46	37	1.00	1.28
0112-017	Q	1.365	-	-0.2	17.4	44	37	0.13	0.60
0113-118	Q	0.670	-	0.1	18.3	3	67	8.74	2.00
0119+041	Q	0.637	0.90	-0.1	19.5	5206	31	0.16	0.30
0133+476	Q	0.860	2.10	0.5	18.0	654	192	0.21	0.24
0146+056	Q	2.345	-	0.8	19.0	17	13	0.22	1.70
0149+218	Q	1.320	1.40	-0.2	18.0	55	15	0.10	0.59
0201+113	G	-	1.30	0.0	19.5	100	18	0.21	0.38
0202+149	Q	-	3.20	-0.4	21.9	1069	135	0.12	0.80
0202+319	Q	1.466	1.60	0.1	18.0	81	3	0.37	0.52
0212+735	Q	-	2.30	-0.1	19.0	30517	374	2.64	1.08
0224+671	Q	-	1.20	0.3	19.5	741	223	2.06	1.20
0229+131	Q	2.065	2.00	-0.5	17.7	14699	30	0.16	0.24
0234+285	Q	1.207	-	-	18.5	16667	472	0.17	0.24
0235+164	Q	0.524	2.10	0.6	19.0	1128	307	0.16	0.24
0237-233	Q	2.223	-	-0.7	16.6	26	3	1.83	8.83
0239+108	Q	-	1.80	0.0	20.0	28	83	0.07	0.93
0256+075	A	-	0.70	0.7	18.0	39	33	0.23	0.22
0300+470	L	-	-	-	18.0	10938	347	0.19	0.24
0309+411	G	-	0.60	0.1	18.0	13	12	0.93	0.22
0316+413	A	0.017	24.80	1.0	12.0	592	38	1.22	1.97
0326+277	Q	1.533	-	-	-	11	10	0.61	0.07
0332-403	Q	1.445	-	0.5	18.5	18	49	0.10	0.14
0333+321	Q	1.258	2.30	-	17.5	84	124	0.25	0.30
0336-019	Q	0.852	2.70	0.4	18.4	223	75	0.16	0.28
0400+258	Q	2.109	1.40	0.0	18.0	47	8	0.71	0.38
0402-362	Q	1.417	-	0.5	17.2	94	121	1.23	0.07
0406+121	Q	-	-	0.5	22.0	15	97	0.13	0.64
0420-014	Q	0.915	1.00	0.3	17.8	12466	500	0.16	0.25
0430+052	A	0.033	6.40	0.1	15.0	119	44	0.69	0.41
0434-188	B	2.702	1.30	0.3	20.0	150	108	0.18	0.30
0440-003	Q	0.850	-	-0.5	19.2	45	16	0.12	1.17
0451-282	Q	2.560	2.30	0.1	19.0	5	20	1.82	0.39
0454-234	Q	1.009	-	0.3	18.5	3429	3	0.95	8.70
0458-020	Q	2.286	2.00	0.1	18.4	160	3	2.47	5.13
0500+019	-	-	2.00	-0.5	-	20	13	0.62	0.24
0454+844	Q	-	1.30	0.3	16.5	32	84	16.12	0.43
0511-220	Q	-	1.30	0.1	19.5	5	11	2.12	0.73
0528+134	Q	-	-	0.5	20.0	20694	148	0.16	0.24

Table 2. (cont.)

OBJECT	Tp (1)	Redsh.	Flux (Jy)	SP	m_V	GSFC soln Nobs	JPL soln Nobs	IERS σ_α (2)	IERS σ_δ (3)
0537-441	Q	0.894	-	0.1	15.5	88	147	2.29	0.49
0552+398	Q	2.365	3.40	-	18.0	42112	724	0.16	0.24
0605-085	Q	-	-	0.2	18.0	61	16	0.02	1.25
0607-157	Q	0.324	1.00	-0.4	18.0	7	13	0.21	3.31
0657+172	-	-	-	-	-	175	25	0.60	1.42
0723-008	Q	0.127	2.10	-0.4	18.0	72	82	0.14	1.42
0727-115	-	-	-	0.1	-	5948	632	0.17	0.28
0735+178	L	-	2.00	0.1	14.9	84	97	0.41	1.23
0736+017	Q	0.191	2.90	-0.1	16.5	69	22	0.24	1.79
0738+313	Q	0.635	1.90	0.2	17.0	118	17	2.27	3.32
0742+103	-	-	3.90	-0.1	-	3918	336	0.16	0.26
0745+241	Q	-	-	0.5	19.0	304	54	0.46	1.38
0748+126	Q	0.889	2.00	0.5	17.8	25	68	0.38	2.23
0754+100	L	-	-	0.2	14.5	27	16	0.46	1.31
0805-077	Q	-	1.10	-0.4	19.5	19	10	0.35	2.04
0814+425	Q	-	1.60	-0.4	18.5	888	162	0.19	0.26
0823+033	Q	-	1.42	0.9	18.0	695	213	0.16	0.26
0827+243	Q	0.939	1.30	-	17.5	19	18	0.26	1.53
0836+710	Q	-	4.40	-0.3	16.5	39	17	2.58	2.65
0851+202	L	0.306	-	1.3	14.0	31084	573	0.16	0.25
0859-140	Q	1.327	2.90	-0.4	16.6	17	21	0.81	3.00
0859+470	Q	1.402	2.20	-0.1	18.7	223	42	0.48	1.59
0917+449	Q	2.180	-	0.6	19.0	16	2	1.43	0.21
0920-397	Q	-	2.10	-0.2	19.0	17	6	1.69	1.45
0923+392	Q	0.699	4.20	1.0	17.8	36367	532	0.16	0.24
0925-203	Q	0.348	-	-0.2	16.4	19	12	1.40	1.18
1004+141	Q	2.707	0.81	-0.1	19.0	18	18	0.53	1.38
1034-293	L	-	1.30	0.5	18.0	1654	217	0.73	2.46
1055+018	Q	0.890	2.87	0.4	18.0	3606	356	0.16	0.27
1104-445	Q	1.598	-	0.1	18.2	123	141	0.36	0.33
1111+149	Q	0.869	-	0.1	18.0	37	25	0.14	1.00
1116+128	Q	2.118	1.74	-0.3	19.3	19	11	0.07	1.70
1123+264	Q	2.341	0.70	-	17.5	234	137	0.16	0.25
1128+385	Q	-	0.90	-0.2	16.0	26	84	0.12	1.33
1144+402	Q	-	0.90	-0.2	18.5	1816	3	0.23	0.34
1144-379	Q	-	-	1.2	16.2	29	222	0.58	0.72
1145-071	Q	-	0.97	0.2	18.5	11	13	0.45	0.48
1148-001	Q	1.982	2.51	-0.4	17.6	41	25	0.98	1.40
1150+812	Q	-	1.20	-0.1	18.5	173	5	2.53	1.99
1156+295	Q	0.729	1.30	-	15.6	3759	1	0.23	0.34
1219+285	L	-	1.47	-	16.5	108	1	0.55	1.61
1222+037	Q	0.957	0.96	0.1	19.0	93	60	0.21	0.48
1226+023	Q	0.158	-	0.0	12.9	17252	296	0.23	0.29
1228+126	G	- 4	-	-0.6	9.6	31	16	0.93	1.21
1243-072	Q	0.267	0.72	0.6	18.0	20	14	0.38	0.93

Table 2. (cont.)

OBJECT	Tp (1)	Redsh.	Flux (Jy)	SP	m_V	GSFC soln Nobs	JPL soln Nobs	IERS	
								σ_α (2)	σ_δ (3)
1244-255	Q	0.633	1.36	0.9	17.0	62	121	1.48	2.06
1253-055	Q	0.538	11.80	0.4	17.8	1506	155	1.04	2.49
1302-102	Q	0.286	1.03	0.1	14.9	12	19	0.44	0.64
1308+326	L	0.996	-	-	19.0	4620	304	0.16	0.26
1313-333	Q	2.210	1.23	0.5	20.0	47	49	0.43	1.60
1334-127	Q	-	1.94	0.2	18.5	3089	272	0.19	0.32
1342+662	Q	-	-	0.1	20.0	11	35	2.84	0.98
1342+663	Q	-	-	0.1	18.8	44	171	2.19	1.61
1354+195	Q	0.720	1.80	-0.1	16.0	901	151	0.16	0.29
1354-152	Q	-	1.17	0.1	18.5	148	20	1.32	2.37
1404+286	G	0.077	1.70	0.9	14.0	24885	22	0.20	0.31
1406-076	Q	1.494	1.30	0.2	20.0	10	11	0.71	0.81
1418+546	L	-	1.00	0.4	14.5	1499	237	0.23	0.29
1424-418	Q	0.308	2.22	0.7	17.5	93	1	33.88	12.02
1435-218	Q	1.194	-	0.2	17.9	3	1	1.42	50.70
1502+106	Q	1.833	2.03	0.6	19.5	6411	193	0.16	0.31
1504+377	-	-	1.10	0.2	-	11	3	5.43	4.00
1504-166	Q	0.876	2.20	-0.4	18.5	31	64	0.86	2.00
1510-089	Q	0.361	3.14	0.3	16.5	697	253	0.19	0.32
1511-100	Q	-	0.88	0.4	18.5	19	16	1.05	0.46
1514-241	L	0.049	1.90	-0.1	15.0	14	10	1.17	0.96
1519-273	Q	-	0.99	0.2	18.5	61	189	0.22	0.47
1538+149	L	-	1.50	-	15.5	22	2	0.19	5.76
1548+056	Q	-	2.28	0.3	18.0	4241	23	0.19	0.32
1555+001	Q	1.770	0.58	0.2	19.3	57	101	0.09	0.13
1606+106	Q	-	1.00	1.1	18.5	32	2	0.07	14.54
1611+343	Q	1.401	-	0.1	17.5	7671	110	0.16	0.30
1624+416	-	-	1.50	-0.3	-	23	1	4.39	14.54
1622-297	-	-	2.20	0.2	-	24	1	2.75	4.51
1633+382	Q	1.814	2.10	0.8	18.0	8075	214	0.17	0.30
1637+574	Q	0.745	1.40	0.4	17.0	2746	4	2.27	0.07
1638+398	Q	-	1.10	0.1	18.5	412	129	1.21	0.24
1642+690	Q	-	1.70	-0.1	20.5	1478	6	3.24	0.03
1641+399	Q	0.595	7.60	0.4	16.0	27450	468	0.16	0.30
1656+053	Q	0.879	1.61	0.5	16.5	143	22	0.32	0.35
1657-261	-	-	1.10	-0.2	-	46	43	1.31	0.55
1717+178	Q	-	1.00	0.6	18.5	19	26	0.01	0.16
1730-130	Q	0.902	-	-0.1	18.5	3250	275	0.19	0.33
1738+476	Q	-	0.92	0.1	17.5	23	97	1.47	0.49
1739+522	Q	1.375	-	0.6	18.5	10064	6	0.22	0.33
1741-038	Q	-	5.60	0.3	18.5	12475	285	0.18	0.32
1743+173	Q	1.725	0.90	0.1	19.5	21	1	0.37	3.86
1749+701	L	0.760	1.10	0.3	17.0	41	115	2.81	0.62
1749+096	L	-	1.07	-0.2	17.0	2735	55	0.18	0.32
1751+288	Q	-	1.10	-	20.0	41	1	3.88	9.61

Table 2. (cont.)

OBJECT	Tp (1)	Redsh.	Flux (Jy)	SP	m_v	GSFC soln Nobs	JPL soln Nobs	IERS	
								σ_α (2)	σ_δ (3)
1803+784	G	-	2.60	0.3	13.0	37196	21	6.71	0.74
1807+698	A	0.050	3.10	-0.3	14.2	41	253	3.81	0.42
1821+107	Q	1.360	-	0.5	16.0	65	47	0.33	0.50
1845+797	A	0.057	7.30	-0.6	15.0	29	5	10.48	1.00
1908-201	-	-	2.30	-	-	11	35	0.39	2.22
1921-293	Q	0.352	-	-	17.5	3098	165	1.76	0.31
1923+210	-	-	-	-	-	157	44	0.29	0.81
1928+738	Q	0.360	3.00	0.0	15.5	596	9	3.84	0.90
1933-400	Q	-	-	0.3	19.0	15	9	2.06	0.79
1936-155	Q	1.657	1.30	0.2	19.4	1	16	1.02	1.46
1954+513	Q	1.230	1.40	-0.1	18.5	156	5	0.80	1.36
1958-179	Q	0.650	1.12	0.1	17.5	270	129	0.20	0.33
2008-159	Q	1.180	0.60	1.0	18.0	24	24	0.20	2.31
2021+614	Q	-	2.26	0.1	19.0	34	115	1.20	1.04
2030+547	-	-	1.40	-	-	25	17	1.28	1.76
2029+121	Q	-	1.10	0.7	18.5	30	33	0.22	1.25
2113+293	Q	-	1.12	-	19.5	182	100	0.19	0.30
2121+053	Q	1.878	2.47	1.1	17.5	12494	36	0.18	0.31
2128+048	-	-	-	-0.5	-	10	1	1.37	39.87
2128-123	Q	0.501	1.69	0.1	16.0	339	26	0.18	0.32
2131-021	L	0.557	2.20	0.2	19.0	18	32	0.09	1.29
2134+004	Q	1.936	6.50	0.8	18.0	8594	121	0.64	0.92
2144+092	Q	-	0.78	0.2	18.6	100	1	0.21	4.52
2145+067	Q	0.990	3.10	0.5	16.5	3670	307	0.16	0.30
2149+056	-	-	1.06	0.3	-	19	78	0.64	1.91
2155-152	L	-	1.80	0.1	17.5	81	53	0.79	0.57
2200+420	L	0.070	4.20	-0.1	14.5	20559	192	0.20	0.27
2201+315	Q	0.297	2.02	0.2	14.5	159	3	0.27	4.55
2216-038	Q	0.901	1.62	0.7	16.4	6564	96	0.19	0.32
2223-052	Q	1.404	5.20	0.2	18.4	28	93	0.27	0.85
2227-088	Q	1.562	1.30	0.5	18.0	15	20	0.07	1.49
2230+114	Q	1.037	-	-0.5	17.3	736	132	0.16	0.29
2234+282	Q	0.795	0.91	-	19.0	10436	166	0.18	0.28
2243-123	Q	0.630	-	-0.2	17.3	82	130	0.19	0.34
2251+158	Q	0.859	10.50	0.8	16.1	19520	263	0.18	0.29
2253+417	Q	1.476	1.50	-0.3	18.8	104	57	0.21	1.12
2254+074	L	-	0.88	0.9	16.5	37	14	0.19	0.62
2318+049	Q	0.633	-	-0.2	19.0	50	31	0.34	1.46
2319+272	G	0.120	1.10	-	15.5	23	3	0.29	0.70
2328+107	Q	1.498	1.05	-0.1	18.1	57	2	0.09	0.73
2344+092	Q	0.677	1.90	-0.2	16.0	20	3	0.17	0.26
2345-167	Q	0.600	-	1.3	18.0	626	74	0.21	0.32
2351+456	G	-	-	-0.1	19.9	18	1	16.50	11.39
2355-106	Q	-	-	0.5	18.0	106	42	0.01	0.71

(1) Type of object: Q :Quasar; G: Galaxy; L: BL Lac; B: Blue object; A: Other.
(2) Unit: 0.0001s
(3) Unit: 0.001"

Table 3. Characteristics of the objects in the IERS Celestial Reference Frame.
Objects observed by one program.

OBJECT	Tp (1)	Redsh.	Flux (Jy)	SP	m_V	GSFC solution Nobs	σ_α (2)	σ_δ (3)	JPL solution Nobs	σ_α (2)	σ_δ (3)
0007+106	Q	0.089	-	-	15.4	19	0.5	0.9			
0013-005	A	-	-	-	19.8				15	0.2	0.5
0014+813	Q	-	1.00	-0.2	16.5	13	29.1	0.6			
0019+058	Q	-	-	0.2	19.5				52	0.3	0.8
0026+346	Q	-	1.80	-0.3	-	22	1.4	1.5			
0047-579	Q	1.797	-	0.4	18.5	2	1.9	3.3			
0056-572	Q	-	-	0.5	18.0	1	7.9	10.5			
0056-001	Q	0.720	2.20	-0.4	17.3	26	0.5	1.5			
0118-272	Q	-	1.00	0.2	16.5	9	0.9	0.6			
0119+115	G	-	1.80	0.3	19.0				29	0.2	0.3
0135-247	Q	0.831	1.49	0.4	16.9	21	0.5	0.3			
0138-097	Q	-	0.90	0.9	18.0	18	0.5	0.4			
0150-334	Q	0.610	1.00	-0.1	16.5	11	0.9	0.7			
0153+744	Q	-	2.10	-0.3	16.0	38	4.6	0.4			
0159+723	-	-	-	0.2	-	20	4.9	0.6			
0202-172	Q	1.740	1.20	0.0	18.0	26	0.4	0.3			
0208-512	Q	1.003	-	-0.2	17.5	139	0.3	0.2			
0220-349	-	-	-	0.0	-	18	0.7	0.4			
0221+067	Q	-	1.40	0.4	20.0				11	0.3	0.4
0230-790	Q	-	-	0.5	18.5	5	26.3	4.7			
0238-084	A	- 5	-	1.5	12.0	25	0.6	0.8			
0241+622	Q	0.044	-	-	15.7	3	21.5	7.0			
0252-549	Q	0.537	-	0.1	18.0	1	1.5	11.5			
0250+178	Q	-	-	0.2	18.5				12	0.4	1.0
0259+121	-	-	-	-	-				1	6.1	64.8
0306+102	L	-	1.30	0.7	20.0				14	0.3	0.4
0308-611	Q	-	-	0.7	18.5	45	1.3	0.4			
0317+188	G	-	-	-0.1	19.0				11	0.2	0.3
0319+121	Q	-	1.40	-0.3	19.0	29	0.3	0.8			
0334-546	Q	-	-	0.2	20.0	1	11.7	12.6			
0338-214	Q	0.048	-	0.2	18.0	16	0.7	0.4			
0342+147	-	-	-	-	-				28	0.3	0.5
0355+508	-	-	6.80	1.0	-	4934	0.2	0.1			
0403-132	Q	0.571	4.00	0.1	17.2	12	0.4	0.4			
0406-127	Q	1.563	-	0.1	18.5				9	0.2	0.5
0409+229	Q	1.213	1.70	-0.4	18.7				13	0.2	0.4
0414-189	Q	1.536	1.00	0.2	18.0	23	0.4	0.4			
0420+417	Q	-	1.70	-	-				15	0.3	0.7
0422+004	L	-	0.80	0.4	16.0	13	0.4	1.0			
0423+233	-	-	-	-	-				11	0.2	0.3
0425+048	Q	-	-	-1.3	20.0				27	1.1	1.5
0426-380	Q	-	1.44	0.2	19.0	27	0.4	0.3			
0426+273	-	-	-	-	-				14	0.2	0.4
0431-512	Q	0.557	-	-0.3	18.0	4	13.1	5.1			
0438-436	Q	2.852	-	0.0	18.8				42	1.1	0.9

Table 3. (cont.)

OBJECT	Tp (1)	Redsh.	Flux (Jy)	SP	m_V	GSFC solution Nobs	GSFC solution σ_α (2)	GSFC solution σ_δ (3)	JPL solution Nobs	JPL solution σ_α (2)	JPL solution σ_δ (3)
0440+345	-	-	-	-	-				13	0.4	0.5
0446+112	G	-	1.80	-	20.0				19	0.3	0.6
0454-810	-	-	-	0.2	-	10	24.5	0.9			
0457+024	Q	2.384	1.30	-0.2	18.0	45	0.3	0.9			
0458+138	-	-	-	0.5	-				9	1.1	1.6
0459+060	Q	-	-	-0.5	19.5				9	0.3	0.6
0502+049	B	-	0.60	0.5	19.0				13	1.0	1.5
0506+101	B	-	4.10	0.2	19.5				21	0.3	0.4
0507+179	-	-	0.70	-	-				26	0.3	0.5
0522-611	Q	1.400	-	-0.1	18.5	4	4.0	1.5			
0530-727	-	-	-	-	-	39	2.8	0.4			
0528-250	Q	2.805	-	-0.2	17.7	22	0.5	0.3			
0529+075	Q	-	1.10	-	19.0	13	3.8	29.0			
0537-158	Q	0.947	-	-0.1	18.0				6	0.5	1.7
0536+145	-	-	-	-	-				30	0.3	0.4
0539-057	Q	-	-	1.4	20.0	10	0.4	1.1			
0544+273	-	-	-	-	-				18	0.5	0.7
0556+238	-	-	-	-	-				42	0.1	0.3
0600+177	-	-	-	-	-				28	0.3	0.4
0611+131	-	-	-	-	-				9	0.1	0.5
0609+607	-	-	-	-	-	60	0.9	0.3			
0615+820	Q	-	1.30	0.0	17.5	12	26.5	1.0			
0629-418	Q	1.416	-	0.5	19.3	16	1.5	0.7			
0637-752	Q	0.651	-	0.1	15.8	175	2.0	0.2			
0637-337	-	-	-	0.4	-	8	1.9	0.6			
0642+214	G	0.245	1.80	-0.7	19.5				16	0.3	0.5
0642+449	Q	3.402	1.20	-0.8	18.5	34	0.4	0.3			
0646-306	-	-	0.90	0.2	-	29	0.4	0.3			
0648-165	-	-	-	-	-	25	0.3	0.3			
0650+371	Q	1.982	1.00	0.4	18.0				1	15.2	15.4
0707+476	Q	-	0.80	-0.3	16.0	31	0.6	0.4			
0710+439	G	-	2.00	-0.2	19.8				1	15.6	16.8
0711+356	Q	1.620	1.90	-0.3	19.0	74	0.4	0.5			
0716+714	L	-	0.70	0.1	11.0	280	0.9	0.2			
0722+145	B	-	5.30	0.0	19.0				17	0.3	0.5
0718+792	-	-	1.00	0.0	-	39	10.3	0.5			
0738-674	-	-	-	-	-	1	28.4	9.5			
0743-006	Q	-	-	0.6	17.5	18	0.3	0.9			
0743+259	-	-	0.60	-	-				16	0.3	0.6
0749+540	Q	-	-	-0.3	18.5	19	1.1	0.7			
0804+499	Q	0.351	1.30	0.5	17.5	62	0.4	0.2			
0809-493	-	-	-	-0.3	-	5	7.0	3.4			
0808+019	L	-	0.39	0.4	17.5	11	0.3	1.0			
0812+367	Q	1.025	1.20	0.0	18.0	39	0.4	0.5			
0818-128	L	-	0.90	-0.1	15.5	15	0.5	0.3			

Table 3. (cont.)

						GSFC solution			JPL solution		
OBJECT	Tp (1)	Redsh.	Flux (Jy)	SP	m_v	Nobs	σ_α (2)	σ_δ (3)	Nobs	σ_α (2)	σ_δ (3)
0820+560	Q	1.409	1.70	-0.1	18.0	101	0.5	0.2			
0823-223	Q	-	-	0.3	17.5	12	0.8	1.7			
0826-373	-	-	2.30	-	-	18	0.8	0.6			
0828+493	Q	-	0.50	-0.3	18.5	63	0.8	0.4			
0834-201	Q	2.752	3.30	-0.1	19.0	19	0.5	1.1			
0833+585	Q	2.101	-	1.3	18.0	38	1.3	0.3			
0839+187	Q	0.259	2.20	0.2	16.5	20	0.4	0.7			
0906+015	Q	1.018	0.76	-0.2	17.5	46	0.4	1.1			
0912+029	Q	-	0.68	-0.3	18.5				16	0.5	0.7
0919-260	Q	2.300	1.20	0.2	19.0	287	0.1	0.2			
0917+624	Q	-	1.60	0.2	19.5	87	0.7	0.2			
0952+179	Q	1.472	1.00	-0.3	18.0				7	0.3	3.0
0953+254	Q	0.712	1.30	1.3	17.5	153	0.1	0.2			
0955+326	Q	0.533	0.70	-0.3	15.8	21	0.4	0.5			
0954+658	Q	-	0.90	0.4	18.5	1622	0.4	0.1			
0959-443	Q	0.021	-	-0.1	17.0	6	4.7	2.6			
1012+232	Q	0.565	-	-0.3	17.5				20	0.3	0.4
1020+400	Q	-	1.20	-0.3	17.5	13	0.7	0.6			
1022+194	Q	0.828	1.04	0.7	17.5				14	0.2	0.5
1030+415	Q	1.120	0.80	0.3	18.2	26	0.6	0.5			
1032-199	Q	2.198	-	0.1	19.0	8	0.6	0.5			
1031+567	Q	-	1.80	-0.3	20.3	11	2.8	1.1			
1038+064	Q	1.270	1.64	-0.4	16.5				68	0.3	0.6
1040+123	Q	1.029	2.38	-0.7	17.3				13	0.2	0.5
1039+811	Q	-	-	0.4	16.5	20	10.2	0.4			
1042+071	B	-	-	0.0	18.5				14	0.3	0.7
1045-188	Q	-	-	0.3	19.0	6	0.7	0.6			
1044+719	-	-	1.00	0.1	-				15	1.0	0.5
1048-313	-	-	0.50	-0.1	-	22	0.5	0.4			
1053+815	G	-	0.60	-0.4	18.5	40	10.4	0.4			
1057-797	-	-	-	0.6	-	174	4.4	0.2			
1101-325	Q	0.354	0.80	-0.4	16.3	266	4.6	84.7			
1101-536	Q	1.598	-	-	18.2	2	2.2	4.6			
1124-186	A	-	0.60	0.5	18.5	100	0.1	0.3			
1127-145	Q	1.187	-	0.2	16.9				60	0.5	0.8
1130+009	Q	-	0.33	0.0	19.0	27	0.5	1.6			
1143-245	Q	1.950	1.10	-0.2	18.0	27	0.5	0.4			
1148-671	-	-	-	-0.6	-	5	11.4	2.5			
1156-094	A	-	0.87	-0.2	-				9	4.8	6.3
1206-399	Q	0.966	-	-0.2	16.1	9	4.6	1.4			
1213-172	-	-	1.20	0.3	-	11	0.4	0.7			
1216+487	Q	1.073	0.70	0.2	18.5	41	0.6	0.4			
1221+809	Q	-	-	-0.3	19.0	54	11.4	0.5			
1221-829	-	-	-	-0.8	-	416	3.6	4.0			
1236-684	-	-	-	-0.5	-	6	16.1	2.9			

Table 3. (cont.)

OBJECT	Tp (1)	Redsh.	Flux (Jy)	SP	m_v	GSFC solution Nobs	GSFC solution σ_α (2)	GSFC solution σ_δ (3)	JPL solution Nobs	JPL solution σ_α (2)	JPL solution σ_δ (3)
1252+119	Q	0.871	1.80	0.2	16.6	54	0.4	0.6			
1251-713	-	-	-	0.2	-	9	5.5	0.7			
1255-316	Q	1.924	1.58	0.1	18.7	25	0.5	0.4			
1315+346	B	1.050	-	-0.1	19.0				8	0.3	1.0
1323+321	G	-	3.60	-0.6	19.0	5	5.3	9.5			
1334-649	-	-	-	0.0	-	5	12.4	2.4			
1349-439	L	0.053	-	0.6	17.5				47	1.4	1.1
1357+769	Q	-	-	0.7	19.0	24	6.0	0.5			
1413+135	G	-	0.90	-0.1	20.0	20	0.4	0.9			
1430-178	Q	2.331	1.19	-0.1	19.5				27	0.6	1.0
1435+638	Q	2.060	1.60	-0.2	15.0	42	1.6	0.4			
1442+101	Q	3.530	2.01	-0.6	17.8	16	0.7	1.2			
1443-162	-	-	-	-	-				8	0.4	0.8
1445-161	A	-	1.01	-0.5	20.5				12	0.4	0.8
1448+762	G	-	1.00	0.5	20.0	21	8.4	0.6			
1451-375	Q	0.314	1.40	0.4	16.2	6	2.7	2.3			
1451-400	-	-	-	-0.2	-	14	1.0	0.6			
1532+016	Q	1.420	1.19	0.3	18.5				20	0.3	0.7
1547+507	Q	-	-	0.1	18.5	32	0.7	0.4			
1546+027	Q	0.412	0.79	0.4	18.0	49	0.3	0.8			
1540-828	-	-	-	0.1	-	32	43.3	3.3			
1549-790	G	-	-	-0.2	20.7	9	15.5	0.7			
1600+335	-	-	2.70	-	-				2	0.9	4.2
1607+268	Q	-	3.10	-0.9	19.0	9	12.3	31.3			
1614+051	Q	3.208	0.63	0.4	19.5				16	0.3	0.7
1610-771	Q	1.710	-	0.8	19.0	137	3.1	0.2			
1619-680	-	-	-	0.0	-	3	4.3	1.8			
1622-253	G	-	-	-0.1	21.3	2273	0.1	0.2			
1652+398	L	0.034	-	0.0	13.8	55	0.3	0.3			
1655+077	Q	-	1.63	0.4	19.5				34	0.3	0.7
1706-174	A	-	-	-	17.5				43	0.5	1.0
1727+502	G	0.055	0.23	-	16.5	1	70.7	41.9			
1732+389	G	-	-	0.8	19.5	60	0.4	0.3			
1758-651	-	-	-	0.1	-	5	15.3	3.5			
1815-553	-	-	-	-0.1	-	140	0.5	0.3			
1826+796	-	-	-	-	-	26	9.7	0.7			
1823+568	Q	-	1.60	0.2	18.4	309	0.3	0.2			
1831-711	Q	1.356	-	-0.2	17.5	18	3.2	0.6			
1842+681	Q	-	1.20	-0.4	17.9	34	1.7	0.3			
1856+736	-	-	-	-	-	24	4.4	0.6			
1903-802	Q	-	-	0.2	19.0	4	26.2	1.0			
1920-211	-	-	-	-	-				44	0.3	0.8
1925-610	-	-	-	-0.1	-	3	2.7	2.3			
1935-692	Q	3.170	-	-	18.8	3	7.4	1.6			
1947+079	Q	-	1.00	0.0	18.0	40	0.3	0.9			

Table 3. (cont.)

						GSFC solution			JPL solution		
OBJECT	Tp (1)	Redsh.	Flux (Jy)	SP	m_v	Nobs	σ_α (2)	σ_δ (3)	Nobs	σ_α (2)	σ_δ (3)
2000-330	Q	3.780	1.10	0.8	19.0	8	2.5	1.1			
2007+777	Q	-	1.20	0.9	16.5	84	3.3	0.2			
2005+403	Q	1.736	4.90	-	19.5	15	2.1	2.0			
2005-489	A	-	-	0.2	16.0	5	4.2	2.4			
2017+743	-	-	-	-	-	27	5.4	0.4			
2021+317	-	-	-	-	-	31	0.4	0.4			
2023+336	-	-	-	-	-	8	2.8	3.6			
2037+511	Q	1.690	5.00	-	20.0	1597	0.2	0.1			
2037-253	Q	1.570	0.90	0.3	18.5	9	0.6	0.4			
2051+745	-	-	-	-	-	12	11.8	0.8			
2059-786	-	-	-	-1.3	-	2	56.4	1.5			
2106-413	Q	-	-	0.2	20.0	10	1.3	0.7			
2109-811	G	-	-	0.2	20.0	5	74.5	4.1			
2126-158	Q	3.270	0.90	0.1	17.3	3	0.3	1.1			
2136+141	Q	2.427	1.19	0.0	18.5	87	0.2	0.3			
2142-758	Q	1.139	-	-0.1	17.4	2	23.0	2.0			
2149-307	Q	2.340	1.35	-0.2	17.5	20	0.5	0.3			
2146-783	-	-	-	-0.1	-	6	39.9	2.1			
2150+173	G	-	1.10	0.4	21.0	38	0.3	0.6			
2210-257	Q	1.833	0.90	0.1	19.5	5	5.3	1.7			
2229+695	G	-	-	0.4	19.6				16	1.1	0.5
2233-148	A	-	-	0.3	19.5	6	0.5	0.6			
2245-328	Q	2.268	-	-0.2	18.6				67	0.5	0.8
2252-090	-	-	-	0.1	-				1	29.8	44.7
2254+024	Q	2.090	-	0.2	18.0				21	0.4	0.7
2255-282	Q	0.926	-	0.4	16.7	1953	0.1	0.1			
2312-319	Q	0.284	-	-0.3	18.5	13	0.9	0.6			
2320-035	Q	1.410	0.79	-0.1	18.0				95	0.2	0.5
2325-150	Q	2.465	1.10	0.2	19.0	7	0.6	0.7			
2326-477	Q	1.302	-	0.0	17.0	57	0.3	0.5			
2329-162	Q	1.153	1.20	-0.2	18.5	8	0.5	0.5			
2329-384	Q	1.195	-	-0.2	16.2	12	0.9	0.5			
2331-240	Q	0.048	0.90	0.0	17.0	4	7.6	8.0			
2335-027	Q	1.072	0.65	0.2	19.3				13	0.3	0.6
2351-154	Q	2.665	-	-0.2	17.0				14	0.2	0.6
2352+495	G	0.237	2.30	-0.3	19.0	56	0.6	0.4			
2355-534	Q	1.006	-	0.4	17.8	30	0.6	0.5			

(1) Type of object: Q: Quasar; G: Galaxy; L: BL Lac; B: Blue object; A: Other
(2) Unit: 0.0001s
(3) Unit: 0.001"

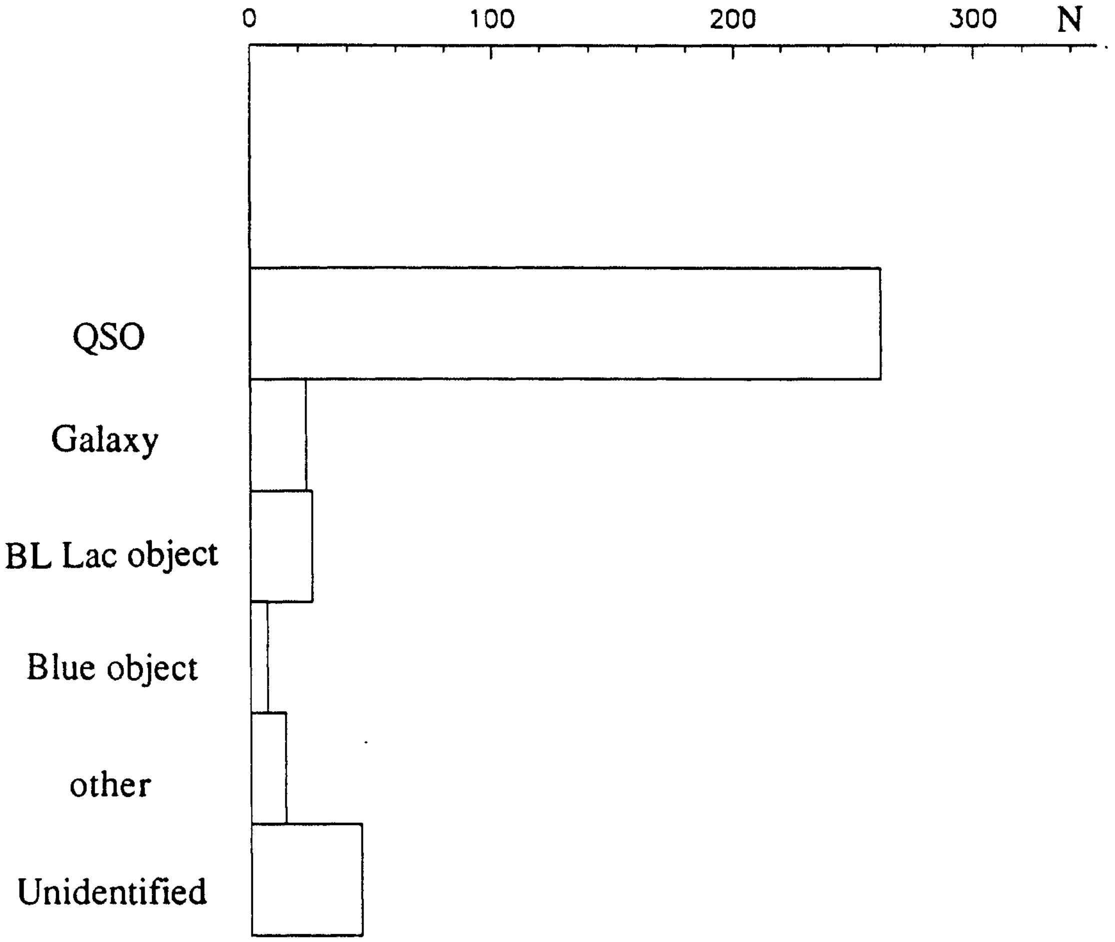

Figure 3a. Optical identification of extragalactic radio sources in RSC(IERS) 91 C 01.

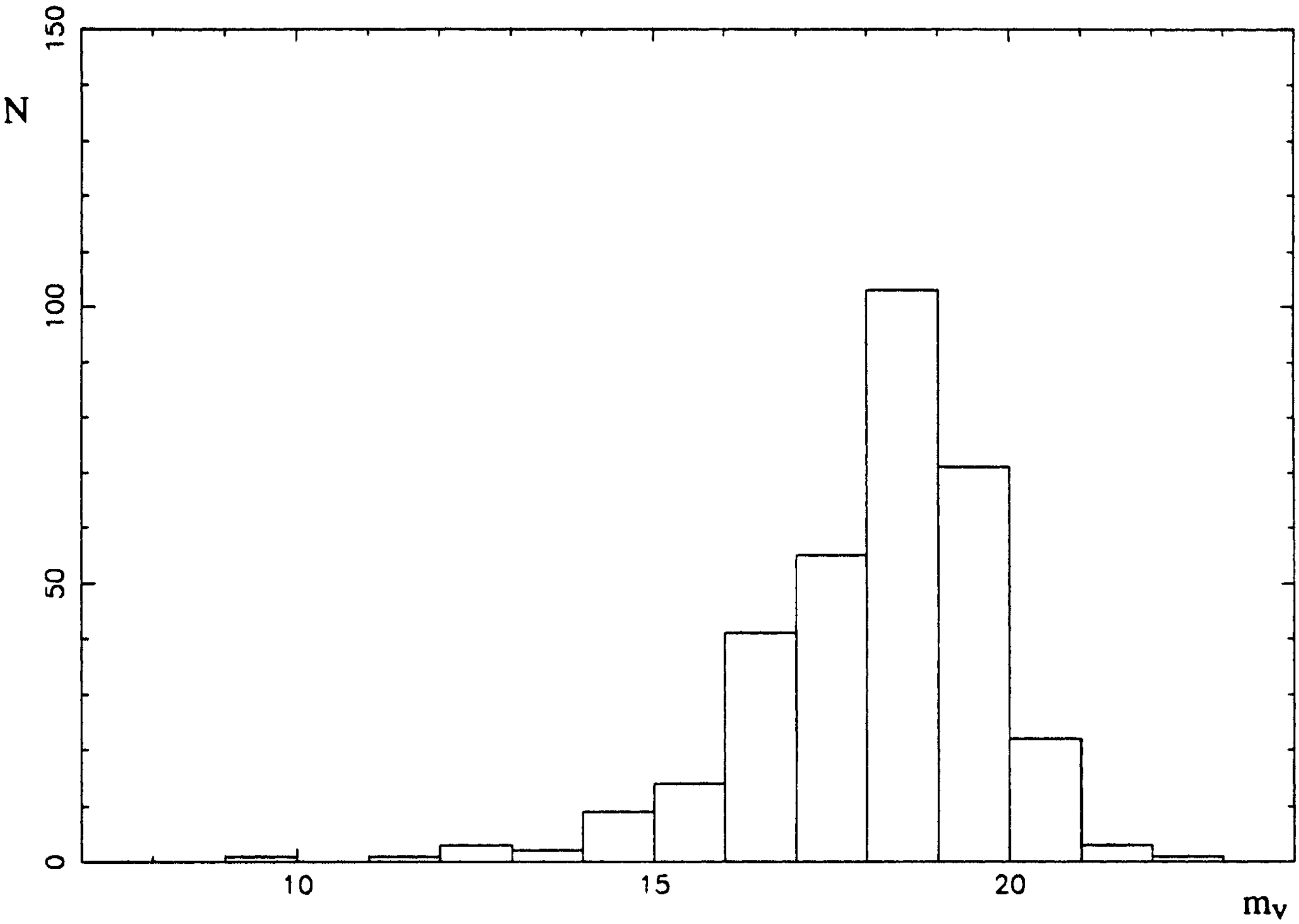

Figure 3b. Visual magnitudes of the optical counterparts of radio sources in RSC(IERS) 91 C 01 (total of 326 values).

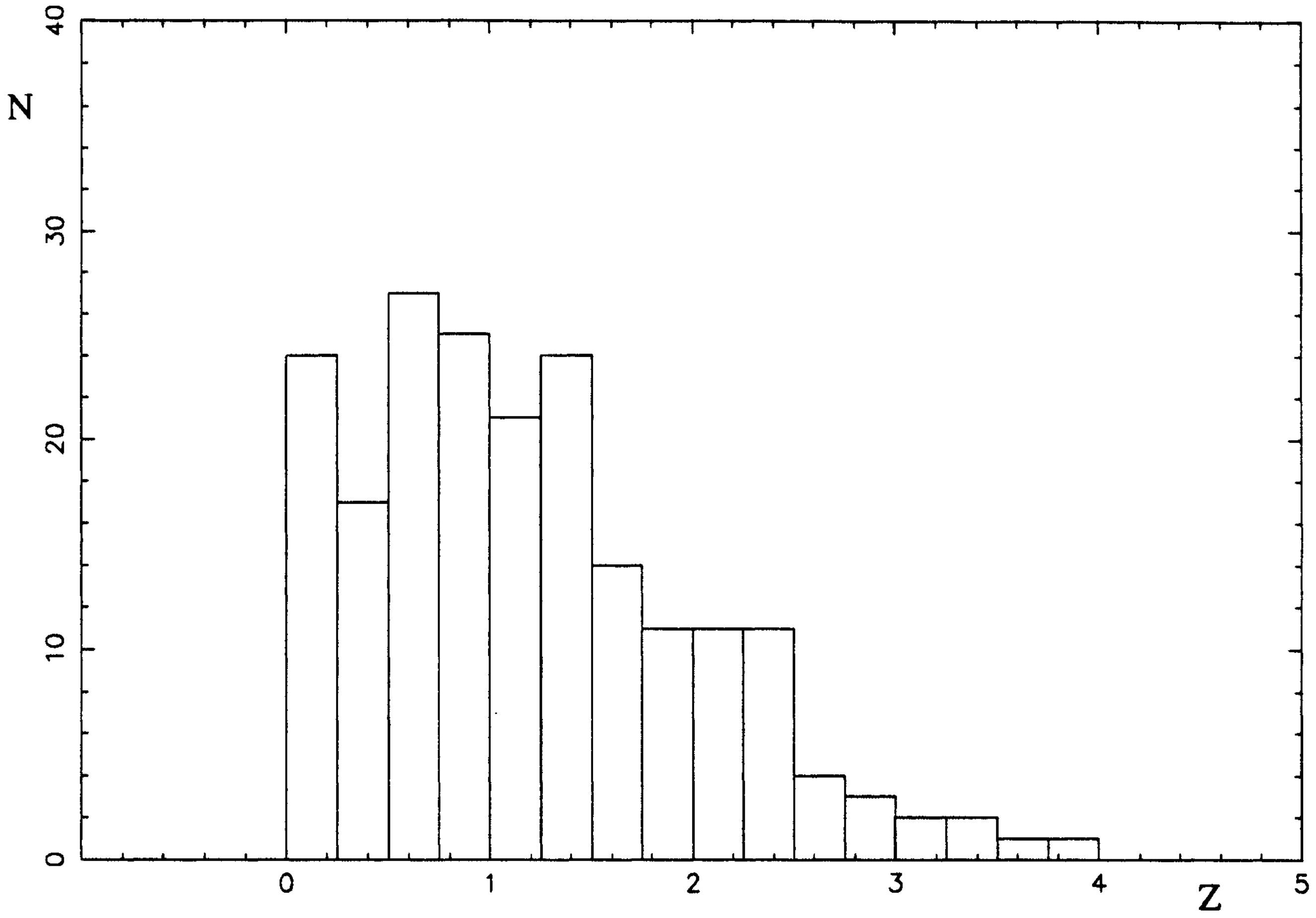

Figure 3c. Redshift of extragalactic radio sources in RSC(IERS) 91 C 01
(total of 198 values).

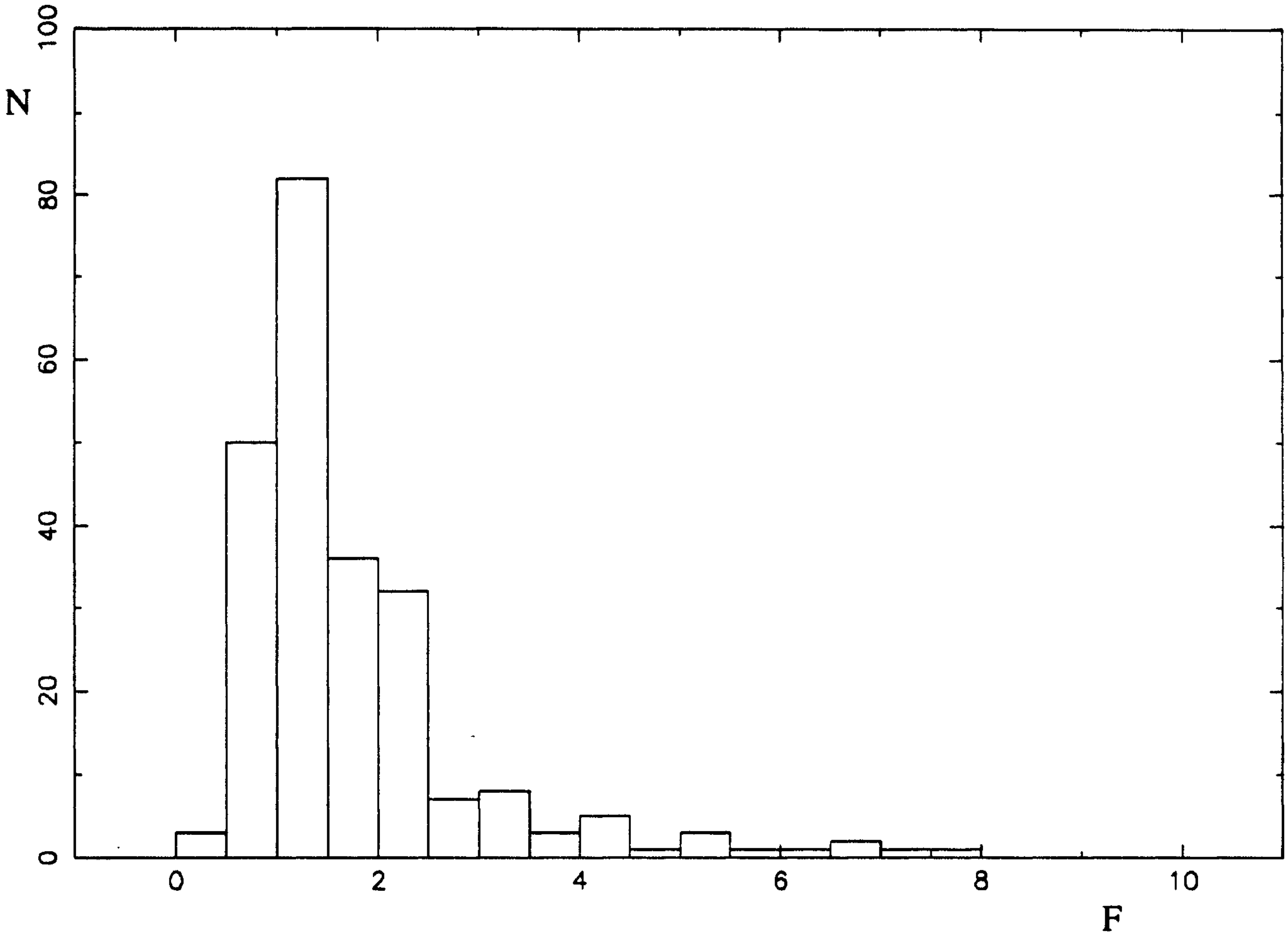

Figure3d. Total flux (Jy) of extragalactic radio sources in RSC(IERS) 91 C 01 (limited to 9.5 Jy; total of 239 values).

Table 4 presents the statistics on the optical identification of radio sources in the IERS frame and in the 917 objects detected in the complete sky survey by Preston *et al.* The distribution of the IERS sources according to their optical classes is similar to the distribution in the survey. Concerning the optical identification of IERS primary sources, 78% of them are quasars, 10% are BL Lac objects and 4% are galaxies. 61% of the quasars selected for the HIPPARCOS/HST link are included in IERS celestial reference frame RSC (IERS) 91 C 01.

Table 4. Optical identifications of the radio sources in the IERS Celestial Reference Frame and in the VLBI survey by Preston *et al.* (1985).

Optical identification (%)	IERS sources (%)	Detected in the survey
Quasar	69	59
Galaxy	7	11
BL Lac	8	7
Stellar objects	4	6
Other/unidentified	12	8
Empty fields		9

Table 5. Distribution of the visual magnitudes of sources in the IERS Celestial Reference Frame

Magnitude range	Number of objects (%)
10 - 12	2
12 - 14	2
14 - 16	6
16 - 18	42
18 - 20	42
20 - 22	6

Table 6. Distribution of the total radio flux of sources in the IERS Celestial Reference Frame.

Flux density (Jy)	Number of objects (%)
0 - 1	22
1 - 2	49
2 - 4	21
4 - 6	4
> 6	4

Table 7. Distribution of redshifts of sources in the IERS Celestial Reference Frame.

Redshift	Number of objects (%)
0 - 1	53
1 - 2	27
2 - 3	17
3 - 4	3

We have also looked at the number of observations of IERS sources in the individual frames of JPL and GSFC contributing to RSC (IERS) 91 C 01. Figures 4a and 4b show the histograms for the number of observations (delay, delay rate) of sources in RSC (JPL) 91 R 01 and in RSC (GSFC) 91 R 04. The total number of sources in each frame is 241 and 334 respectively. The histogram for the number of observations of sources in the last realisation of IERS frame (both individual VLBI frames together) is plotted in Figure 5.

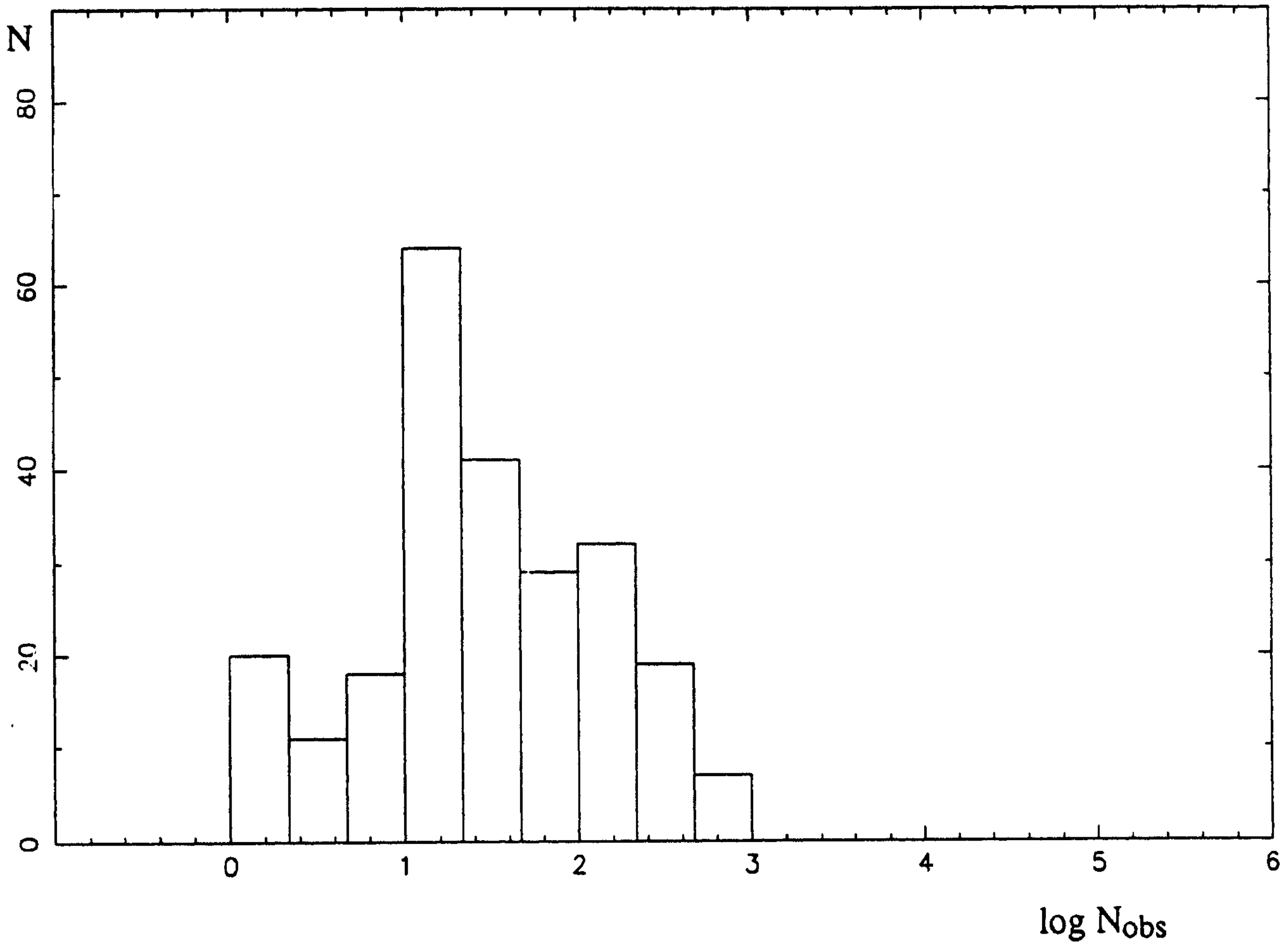

Figure 4a. Number of observations of extragalactic radio sources in RSC (JPL) 91 R 01. The total number of sources in the frame is 241.

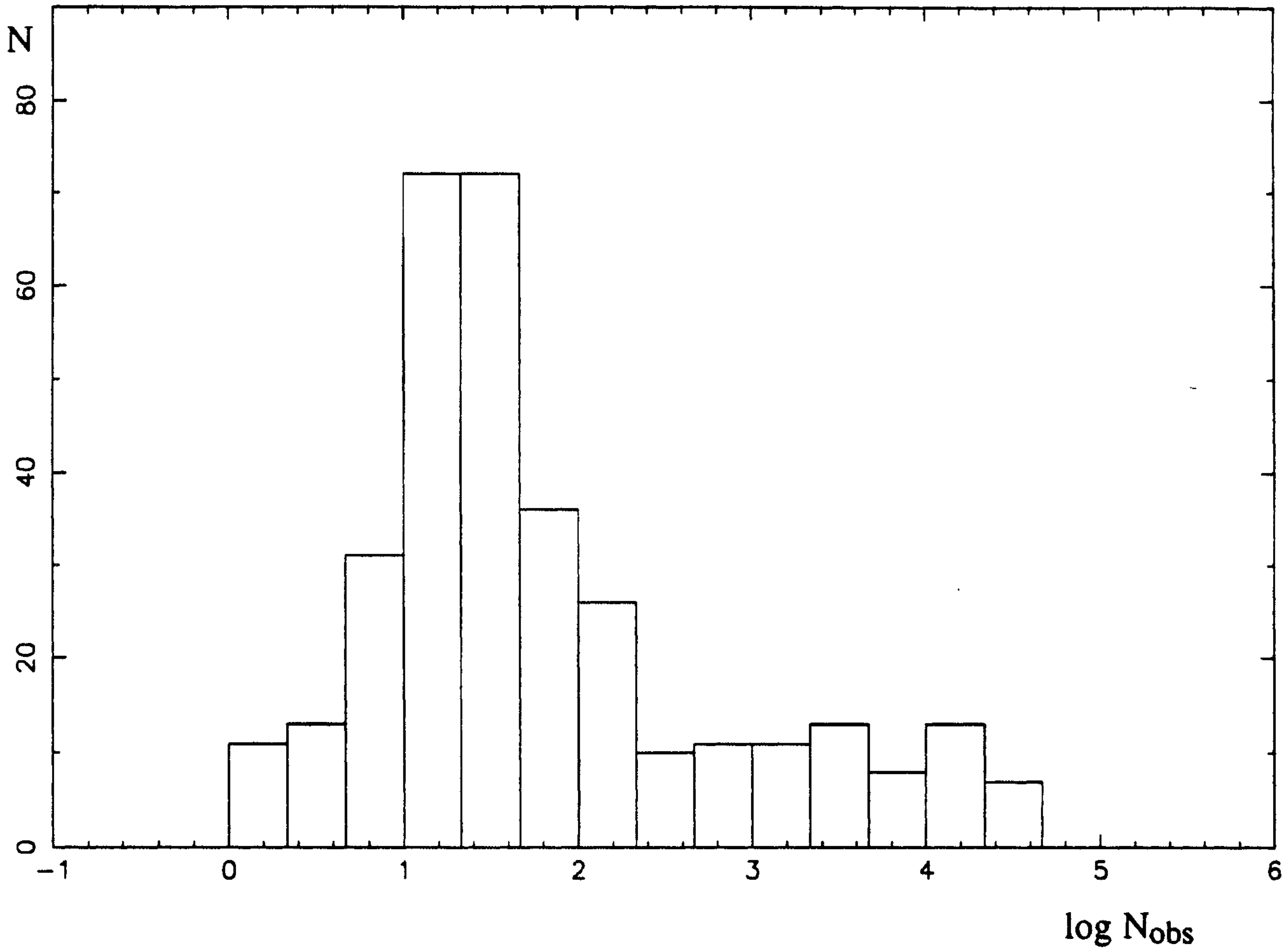

Figure 4b.Number of observations of extragalactic radio sources in RSC (GSFC) 91 R 04. The total number of sources in the frame is 334.

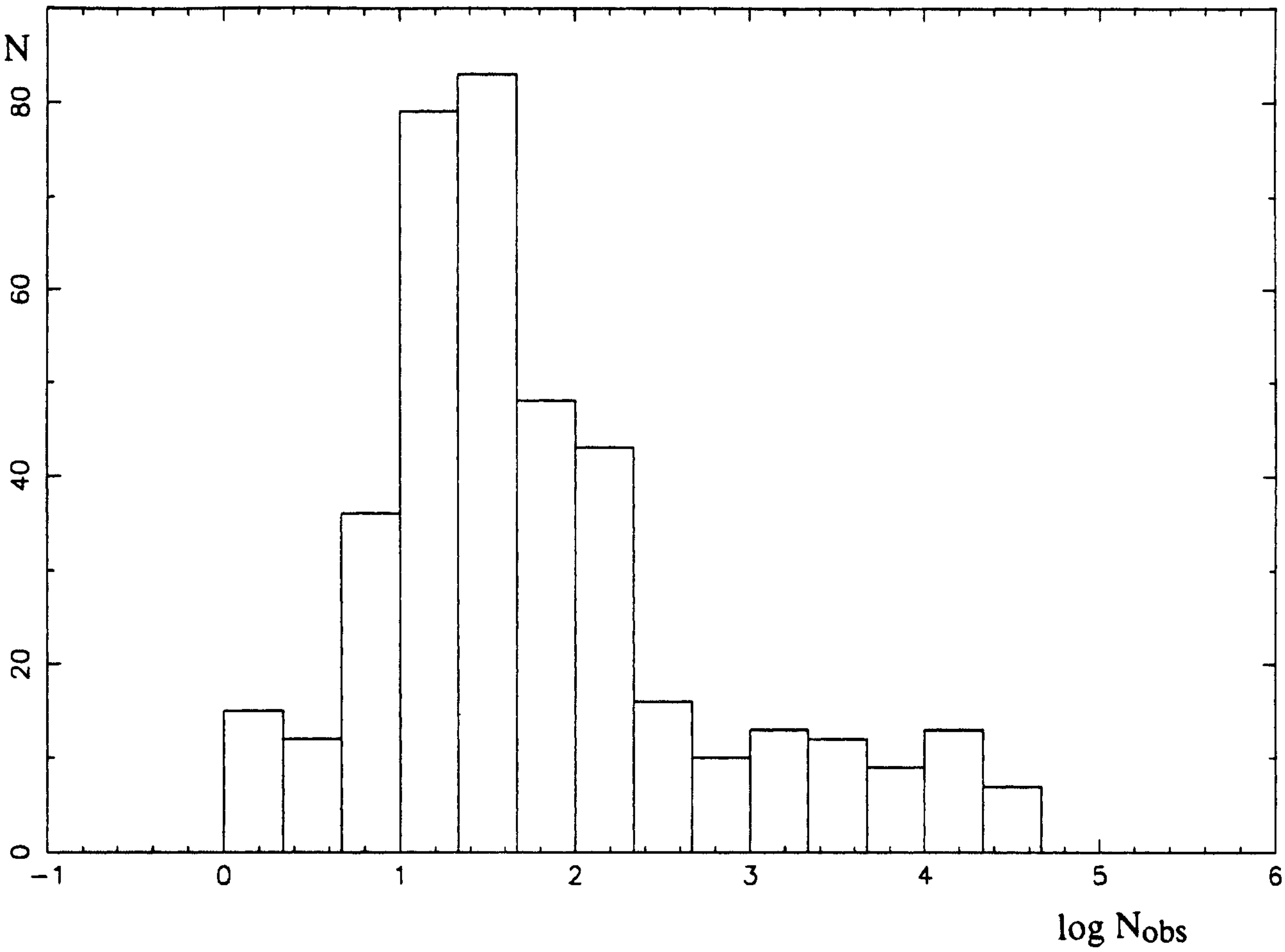

Figure 5. Number of observations of extragalactic radio sources in RSC (IERS) 91 R 01. The total number of sources in the frame is 396.